BASIS PURSUIT FOR SPECTRUM CARTOGRAPHY*

Juan Andrés Bazerque, Gonzalo Mateos and Georgios B. Giannakis

Dept. of ECE, University of Minnesota, 200 Union Street SE, Minneapolis, MN 55455.

ABSTRACT

A nonparametric version of the basis pursuit method is developed for field estimation. The underlying model entails known bases, weighted by generic functions to be estimated from the field's noisy samples. A novel field estimator is developed based on a regularized variational least-squares (LS) criterion that yields estimates spanned by thin-plate splines. Robustness considerations motivate well the adoption of an overcomplete set of basis functions, together with a sparsity-promoting regularization term, which endows the estimator with the ability to select a few of these bases that "better" explain the data. This parsimonious field representation becomes possible because the sparsity-aware spline-based method of this paper induces a group-Lasso estimator of the thin-plate spline basis expansion coefficients. The novel spline-based approach to basis pursuit is motivated by a *spectrum cartography* application, in which a set of sensing cognitive radios collaborate to estimate the distribution of RF power in space and frequency. Simulated tests corroborate that the estimated power spectrum density atlas yields the desired RF state awareness, since the maps reveal spatial locations where idle frequency bands can be reused for transmission, even when fading and shadowing effects are pronounced.

***Index Terms*—** Sparsity, basis pursuit, splines, (group-)Lasso, field estimation, cognitive radio sensing.

1. INTRODUCTION

The unceasing demand for continuous situational awareness in the context of cognitive radio (CR) networks calls for innovative signal processing algorithms, complemented by collaborative sensing platforms to accomplish the objectives of layered sensing and control. These challenges are embraced in the study of *spectrum cartography* whereby CRs cooperate to estimate the distribution of power across spatial locations $\mathbf{x}$ and frequencies f, namely the power spectrum density (PSD) map $\Phi(\mathbf{x}, f)$. Knowing the PSD at any location allows remote CRs to reuse dynamically idle bands. It also reveals additional opportunities compared to existing alternatives, which have mostly relied on space-invariant models for the RF ambience [9], [8]. Indeed, it broadens the access of secondary systems to the RF spectrum, since knowledge of $\Phi(\mathbf{x}, f)$ allows CRs to share frequencies with primary users as long as they operate in areas (spatial holes) where the primary signal is too weak for reliable communication; see also [2].

The estimated PSD map need not be extremely accurate, but precise enough to identify spectrum holes. As it will be argued in Section 2, this justifies adopting a set of known bases to capture the frequency dependence of $\Phi(\mathbf{x}, f)$, yielding the basis expansion model

$$\Phi(\mathbf{x}, f) = \sum_{\nu=1}^{N_b} g_\nu(\mathbf{x}) b_\nu(f) \tag{1}$$

with $\mathbf{x} \in \mathbb{R}^2$, $f \in \mathbb{R}$, and the L_2-norms $\{||b_\nu(f)||_{L_2} = 1\}_{\nu=1}^{N_b}$ normalized to unity. The bases $\{b_\nu(f)\}_{\nu=1}^{N_b}$ are preselected, and the functions $g_\nu(\mathbf{x})$ are to be estimated based on noisy PSD samples. As far as the spatial dependence is concerned, the model must account for path loss, fading, mobility, and shadowing effects, all of which vary with the propagation medium. For this reason, it is prudent to adopt a *nonparametric* approach and let the data dictate the spatial component of (1). This motivates a variational least-squares (LS) estimator for $g_\nu(\mathbf{x})$ regularized with a thin-plate splines penalty, enforcing smoothness in the solution, and rendering it expressible as a combination of radial basis kernels [6].

Consider selecting N_b basis functions using the *basis pursuit* approach [5], which entails an extensive set of bases (N_b overly large) and thus an overcomplete model. This motivates augmenting the variational LS problem with an extra sparsity-encouraging penalty, which endows the map estimator with the ability to discard factors $g_\nu(\mathbf{x})b_\nu(f)$ in (1), only retaining a few bases that "better" explain the data. This attribute is inherited because the novel sparsity-aware spline-based method of this paper induces a group-Lasso estimator for the coefficients of the spline-based representation of g_ν. Group-Lasso estimators are known to set groups of weak coefficients to zero (here the N_b groups associated with coefficients per g_ν), and outperform the sparsity-agnostic LS estimator by capitalizing on the sparsity present [10]. A related approach to model selection in nonparametric regression is the component selection and smoothing operator (COSSO) [7]. Different from the approach followed here, COSSO does not perform basis selection and is limited to smoothing-spline, analysis-of-variance models. Compared to the single group-Lasso estimate here, COSSO entails an iterative algorithm, which alternates through a sequence of smoothing spline and nonnegative garrote subproblems.

2. BEM FOR SPECTRUM CARTOGRAPHY

Consider a set of N_s sources transmitting signals $\{u_s(t)\}_{s=1}^{N_s}$ using portions of the overall bandwidth B. The objective of revealing which of these portions (sub-bands) are available for new systems to transmit, suggests that the PSD estimate sought does not need to be super accurate. This motivates modeling the transmit-PSD of each $u_s(t)$ as

$$\Phi_s(f) = \sum_{\nu=1}^{N_b} \theta_{s\nu} b_\nu(f), \;\; s = 1, \ldots, N_s \tag{2}$$

where the basis $b_\nu(f)$ is centered at frequency f_ν, $\nu = 1, \ldots, N_b$. The example depicted in Fig. 1 involves (generally *overlapping*) raised cosine bases with support $B_\nu = [f_\nu - (1+\rho)/2T_s, f_\nu + (1+\rho)/2T_s]$, where T_s is the symbol period, and ρ stands for the

* Work in this paper was supported by the NSF grants CCF-0830480, CCF-1016605, ECCS-0824007, and ECCS-1002180.

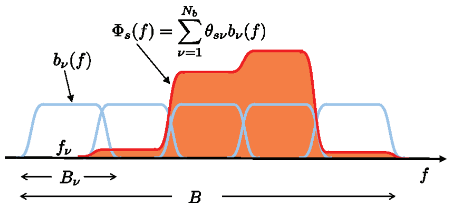

Fig. 1. Expansion with overlapping raised cosine pulses.

roll-off factor. Such bases can model transmit-spectra of e.g., multi-carrier systems. In other situations, power spectral masks may dictate sharp transitions between contiguous sub-bands, cases in which non-overlapping rectangular bases may be more appropriate. All in all, the set of bases should be selected to accommodate a priori knowledge about the PSD.

The power transmitted by source s will propagate to the location $\mathbf{x} \in \mathbb{R}^2$ according to a generally unknown spatial loss function $l_s(\mathbf{x}) : \mathbb{R}^2 \to \mathbb{R}$. The propagation model $l_s(\mathbf{x})$ not only captures frequency-flat deterministic pathloss or frequency-invariant shadowing patterns, but also stationary, block-fading and even frequency-selective Rayleigh channel effects, since their statistical moments do not depend on the frequency variable. In this case, the following vanishing memory assumption is required on the transmitted signals for the spatial receive-PSD $\Phi(\mathbf{x}, f)$ to be factorizable as $l_s(\mathbf{x})\Phi_s(f)$; see [3] for further details.

(as) *Sources $\{u_s(t)\}_{s=1}^{N_s}$ are stationary, mutually uncorrelated, independent of the channels, and have vanishing correlation per coherence interval; i.e., $r_{ss}(\tau) := E[u_s(t+\tau)u_s(t)] = 0, \forall\, |\tau| > T_c - L$, where T_c and L represent the coherence interval and delay spread of the channels, respectively.*

Under (as), the contribution of source s to the PSD at point $\mathbf{x}$ is $l_s(\mathbf{x}) \sum_{\nu=1}^{N_b} \theta_{s\nu} b_\nu(f)$; and the PSD due to all sources received at $\mathbf{x}$ will be given by $\Phi(\mathbf{x}, f) = \sum_{s=1}^{N_s} l_s(\mathbf{x}) \sum_{\nu=1}^{N_b} \theta_{s\nu} b_\nu(f)$. Such a model can be simplified by defining the function $g_\nu(\mathbf{x}) := \sum_{s=1}^{N_s} \theta_{s\nu} l_s(\mathbf{x})$. With this definition and upon exchanging the order of summation, the spatial PSD model takes the form in (1), where functions $\{g_\nu(\mathbf{x})\}_{\nu=1}^{N_b}$ are to be estimated. They represent the aggregate distribution of power across space corresponding to the frequencies spanned by the bases $\{b_\nu\}$. Note that the sources are not explicitly present in (1). Even if this model could have been postulated directly for the cartography task at hand, the previous discussion justifies the factorization of the $\Phi(\mathbf{x}, f)$ map per band in factors depending on each of the variables $\mathbf{x}$ and f.

3. COOPERATIVE SPLINE-BASED PSD ESTIMATION

The sensing strategy will rely on the periodogram estimate $\widehat{\phi}_{rn}(\tau)$ at a set of receiving (sampling) locations $\mathcal{X} := \{\mathbf{x}_r\}_{r=1}^{N_r} \in \mathbb{R}^2$, frequencies $\mathcal{F} := \{f_n\}_{n=1}^{N} \in B$, and time-slots $\{\tau\}_{\tau=1}^{T}$. In order to reduce the periodogram variance and mitigate fading effects, $\widehat{\phi}_{rn}(\tau)$ is averaged across a window of T time-slots [3], to obtain

$$\varphi_{rn} := \frac{1}{T} \sum_{\tau=1}^{T} \widehat{\phi}_{rn}(\tau). \tag{3}$$

Hence, the envisioned setup consists of N_r receiving CRs, which collaborate to estimate the PSD map based on observations $\{\varphi_{rn}\}$.

While a BEM could be introduced for the spatial loss function $l_s(\mathbf{x})$ as well [3], the uncertainty on the source locations and obstructions in the propagation medium may render such a model imprecise. This will happen, e.g., when shadowing is present. The alternative approach followed here relies on estimating $\{g_\nu(\mathbf{x})\}_{\nu=1}^{N_b}$ based on the data $\{\varphi_{rn}\}$. To capture the smooth portions of $\Phi(\mathbf{x}, f)$, the criterion for selecting $g_\nu(\mathbf{x})$ will be regularized using a so termed thin-plate penalty [6]. This penalty extends to $\mathbb{R}^2$ the one-dimensional roughness regularization used in smoothing spline models.

A second penalty term is introduced to fit the unknown spatial functions $\{g_\nu\}_{\nu=1}^{N_b}$ in the model with a large ($N_b \gg N_r N$), and a possibly overcomplete set of known basis functions $\{b_\nu\}_{\nu=1}^{N_b}$. These models are particularly attractive when there is an inherent uncertainty on the transmitters' parameters, such as central frequency and bandwidth of the pulse shapers; or, e.g., the roll-off factor when raised-cosine pulses are employed. In particular, adaptive communication schemes rely on frequently adjusting these parameters. A sizeable collection of bases to effectively accommodate most of the possible cases provides the desirable robustness. Still, prior knowledge available on the incumbent communication technologies being sensed should be exploited to choose the most descriptive classes of basis functions; e.g., a large set of raised-cosine pulses. This knowledge justifies why known bases are selected to describe frequency characteristics of the PSD map, while a variational approach is preferred to capture spatial dependencies.

In this context, the envisioned estimation method should provide the CRs with the capability of selecting a *few* bases that "better explain" the actual transmitted signals. As a result, most functions g_ν are expected to be identically zero; hence, there is an inherent form of sparsity present that can be exploited to improve estimation. The rationale behind the proposed approach is rooted in the *basis pursuit* principle, a term coined by [5] for finding the most parsimonious sparse signal expansion using an overcomplete basis set. A major differentiating aspect however, is that while the sparse coefficients in the basis expansions treated in [5] are scalars, model (1) here entails basis functions weighted by coefficient functions g_ν.

Accordingly, the proposed approach to sparsity-aware spline-based field estimation from the space-frequency PSD measurements φ_{rn} [cf. (3)], is to obtain $\{\hat{g}_\nu\}_{\nu=1}^{N_b}$ as

$$\{\hat{g}_\nu\}_{\nu=1}^{N_b} := \arg\min_{\{g_\nu \in \mathcal{S}\}} \left[\frac{1}{N_r N} \sum_{r=1}^{N_r} \sum_{n=1}^{N} \left(\varphi_{rn} - \sum_{\nu=1}^{N_b} g_\nu(\mathbf{x}_r) b_\nu(f_n) \right)^2 \right.$$
$$\left. + \lambda \sum_{\nu=1}^{N_b} \int_{\mathbb{R}^2} ||\nabla^2 g_\nu(\mathbf{x})||_F^2 d\mathbf{x} + \mu \sum_{\nu=1}^{N_b} \left\| [g_\nu(\mathbf{x}_1), \ldots, g_\nu(\mathbf{x}_{N_r})]' \right\|_2 \right] \tag{4}$$

where $||\nabla^2 g_\nu||_F$ denotes the Frobenius norm of the Hessian of g_ν. The optimization is over $\mathcal{S}$, the space of Sobolev functions, for which the thin-plate penalty is well defined [6]. The parameter $\lambda \geq 0$ included in this penalty controls the degree of smoothing. Specifically, for $\lambda = 0$ the estimates in (4) correspond to *rough* functions interpolating the data; while as $\lambda \to \infty$ the estimates yield linear functions (cf. $\nabla^2 \hat{g}_\nu(\mathbf{x}) \equiv \mathbf{0}_{2\times 2}$). A smoothing parameter in between these limiting values is selected using a leave-one-out cross-validation (CV) approach.

The additional regularization term, which is weighted by a tuning parameter $\mu \geq 0$, is responsible for the sparsity in the solution. Note that the minimization of $\left\| [g_\nu(\mathbf{x}_1), \ldots, g_\nu(\mathbf{x}_{N_r})]' \right\|_2$ intuitively shrinks all pointwise functional values $\{g_\nu(\mathbf{x}_1), \ldots, g_\nu(\mathbf{x}_{N_r})\}$ to zero for sufficiently large μ. Interestingly, it will be shown in the ensuing section that this is enough to guarantee that $\hat{g}_\nu(\mathbf{x}) \equiv 0\ \forall \mathbf{x}$, for μ large enough.

4. GROUP-LASSO ON SPLINES

The optimization problem (4) is variational in nature, and in principle requires searching over the infinite-dimensional functional space $\mathcal{S}$. It turns out that (4) admits closed-form, finite dimensional minimizers $\hat{g}_\nu(\mathbf{x})$, as presented in the following proposition, which provides a generalization of the standard thin-plate splines results [6], to the multi-dimensional BEM (1) [4].

Proposition 1: *The estimates $\{\hat{g}_\nu\}_{\nu=1}^{N_b}$ in* (4) *are thin-plate splines expressible in closed form as*

$$\hat{g}_\nu(\mathbf{x}) = \sum_{r=1}^{N_r} \beta_{\nu r} K(||\mathbf{x}-\mathbf{x}_r||_2) + \boldsymbol{\alpha}_{\nu 1}'\mathbf{x} + \alpha_{\nu 0} \tag{5}$$

where $K(\rho) := \rho^2 \log(\rho)$, and $\boldsymbol{\beta}_\nu := [\beta_{\nu 1}, \ldots, \beta_{\nu N_r}]'$ is constrained to the linear subspace $\mathcal{B} := \{\boldsymbol{\beta} \in \mathbb{R}^{N_r} : \sum_{r=1}^{N_r} \beta_r = 0, \sum_{r=1}^{N_r} \beta_r \mathbf{x}_r = \mathbf{0}_2,\ \mathbf{x}_r \in \mathcal{X}\}$ for $\nu = 1, \ldots, N_b$.

4.1. Estimation using the group-Lasso

Consider the classical problem of linear regression where a vector $\mathbf{y} \in \mathbb{R}^n$ of observations is available, along with a matrix $\mathbf{X} \in \mathbb{R}^{n\times p}$ of inputs. The group-Lasso estimate for the vector of features $\boldsymbol{\zeta} := [\boldsymbol{\zeta}_1', \ldots, \boldsymbol{\zeta}_{N_b}']' \in \mathbb{R}^p$ is defined as the solution to [10]

$$\min_{\boldsymbol{\zeta}} \frac{1}{2}\|\mathbf{y} - \mathbf{X}\boldsymbol{\zeta}\|_2^2 + \mu \sum_{\nu=1}^{N_b} \|\boldsymbol{\zeta}_\nu\|_2. \tag{6}$$

This criterion achieves model selection by retaining relevant factors $\boldsymbol{\zeta}_\nu \in \mathbb{R}^{p/N_b}$ in which the features are grouped. In other words, group-Lasso encourages sparsity at the factor level, either by shrinking to zero all variables within a factor, or by retaining them altogether depending on the value of the tuning parameter $\mu \geq 0$. As μ is increased, more sub-vector estimates $\boldsymbol{\zeta}_\nu$ become zero, and the corresponding factors drop out of the model.

The connection between (6) and the spline-based field estimator (4) builds on Proposition 1, and is revealed when estimating the parameters $\boldsymbol{\alpha}_\nu$ and $\boldsymbol{\beta}_\nu$ in (5), as presented in Proposition 2. To this end, some definitions are due at this point. Consider the vector $\boldsymbol{\varphi} := [\varphi_{11}, \ldots, \varphi_{1N}, \ldots, \varphi_{N_r 1}, \ldots, \varphi_{N_r N}]' \in \mathbb{R}^{N_r N}$ containing the network-wide data obtained at all frequencies in $\mathcal{F}$. Three matrices are also introduced collecting the regression inputs: i) $\mathbf{T} \in \mathbb{R}^{N_r \times 3}$ with rth row $\mathbf{t}_r' := [1\ \mathbf{x}_r']$ for $r = 1, \ldots, N_r$ and $\mathbf{x}_r \in \mathcal{X}$; ii) $\mathbf{B} \in \mathbb{R}^{N\times N_b}$ with nth row $\mathbf{b}_n' := [b_1(f_n), \ldots, b_{N_b}(f_n)]$ for $n = 1, \ldots, N$; and iii) $\mathbf{K} \in \mathbb{R}^{N_r\times N_r}$ with ij-th entry $[\mathbf{K}]_{ij} := K(||\mathbf{x}_i - \mathbf{x}_j||)$ for $\mathbf{x}_i, \mathbf{x}_j \in \mathcal{X}$. Consider also the QR decomposition of $\mathbf{T} = [\mathbf{Q}_1\ \mathbf{Q}_2]\,[\mathbf{R}'\ \mathbf{0}]'$.

These matrices are involved in obtaining the optimal $\boldsymbol{\alpha}_\nu$ and $\boldsymbol{\beta}_\nu$ as summarized in the following result [4].

Proposition 2: *The spline-based field estimator* (4) *is equivalent to group-Lasso* (6)*, under the identities*

$$\mathbf{y} := \frac{1}{\sqrt{N_r N}}[\boldsymbol{\varphi}',\ \mathbf{0}]'$$

$$\mathbf{X} := \frac{\begin{bmatrix} \mathbf{B}\otimes \mathbf{I}_{N_r} \\ \mathbf{I}_{N_b} \otimes \left\{ bdiag((N_r N \lambda \mathbf{Q}_2'\mathbf{K}\mathbf{Q}_2)^{1/2}, \mathbf{0})[\mathbf{K}\mathbf{Q}_2\ \ \mathbf{T}]^{-1}\right\} \end{bmatrix}}{\sqrt{N_r N}} \tag{7}$$

with their respective solutions related by (5) *and*

$$[\boldsymbol{\beta}_\nu', \boldsymbol{\alpha}_\nu']' = bdiag(\mathbf{Q}_2, \mathbf{I}_3)[\mathbf{K}\mathbf{Q}_2\ \ \mathbf{T}]^{-1}\hat{\boldsymbol{\zeta}}_\nu \tag{8}$$

where $\boldsymbol{\alpha}_\nu := [\alpha_{\nu 0}, \boldsymbol{\alpha}_{\nu 1}']'$.

Factors $\{\boldsymbol{\zeta}_\nu\}_{\nu=1}^{N_b}$ in (6) are in one-to-one correspondence with vectors $\{[\boldsymbol{\beta}_\nu', \boldsymbol{\alpha}_\nu']'\}_{\nu=1}^{N_b}$ through the linear mapping (8). This implies that whenever a factor $\boldsymbol{\zeta}_\nu$ is dropped from the linear regression model obtained after solving (6), then $\hat{g}_\nu(\mathbf{x}) \equiv 0$, and the term corresponding to $b_\nu(f)$ does not contribute to (1). Hence, by appropriately selecting the value of μ, criterion (4) has the potential of retaining only the most significant terms in $\Phi(\mathbf{x}, f) = \sum_{\nu=1}^{N_b} g_\nu(\mathbf{x}) b_\nu(f)$, and thus yields parsimonious PSD map estimates. All in all, the motivation behind the variational problem (4) is now unravelled. The second penalty renders (4) equivalent to a group-Lasso problem. This enforces sparsity in the parameters of the splines expansion for $\Phi(\mathbf{x}, f)$ at a factor level, which is exactly what is needed to potentially null the less descriptive functions g_ν.

The group-Lassoed splines-based approach to spectrum cartography developed in this section can be summarized in the following steps to estimate the global PSD map $\Phi(\mathbf{x}, f)$:

S1. Given $\boldsymbol{\varphi}$, compute (7), and solve (6) for $\hat{\boldsymbol{\zeta}} := [\hat{\boldsymbol{\zeta}}_1', \ldots, \hat{\boldsymbol{\zeta}}_{N_b}']'$.

S2. Change variables $[\hat{\boldsymbol{\beta}}_\nu', \hat{\boldsymbol{\alpha}}_\nu']' = \text{bdiag}(\mathbf{Q}_2, \mathbf{I}_3)[\mathbf{K}\mathbf{Q}_2\ \ \mathbf{T}]^{-1}\hat{\boldsymbol{\zeta}}_\nu$.

S3. Substitute $\hat{\boldsymbol{\alpha}}_{\boldsymbol{\nu}}$ and $\hat{\boldsymbol{\beta}}_{\boldsymbol{\nu}}$ into (5) to obtain $\{\hat{g}_\nu(\mathbf{x})\}_{\nu=1}^{N_b}$.

S4. Use $\{\hat{g}_\nu(\mathbf{x})\}_{\nu=1}^{N_b}$ in (1) to estimate $\Phi(\mathbf{x}, f)$.

5. NUMERICAL TESTS

Consider a set of $N_r = 100$ CRs uniformly distributed in an area of 100m^2, cooperating to estimate the PSD map generated by $N_s = 2$ licensed users (sources). Both transmitted signals are raised cosine pulses with roll-off factors $\rho = 1$ and $\rho = 0$, respectively, and corresponding bandwidths $W = 10$ and $W = 20$ MHz. They share the frequency band $B = [100, 200]$ MHz with spectra centered at frequencies $f_c = 115$ and 165MHz, respectively. Fig. 2 (top) depicts the PSD generated by the active transmitters. The PSD generated by source s experiences fading and shadowing effects in its propagation from $\mathbf{x}_s$ to any location $\mathbf{x}$, where it can be measured in the presence of noise. A 6-tap Rayleigh model is adopted for the multipath channel $H_s(f, \tau, \mathbf{x})$ between $\mathbf{x}_s$ and $\mathbf{x}$, whose expected gain adheres to the path-loss law $E(|H_s|^2) = \min\left\{(1, (\Delta/||\mathbf{x}_s - \mathbf{x}||_2)^3\right\}$, with $\Delta = 60m$. Shadowing effects are simulated using the model in [1] with $\sigma = 5dB$ and $\delta = 25$m. The combined propagation pattern for the power transmitted by source TX_1 is depicted in Fig. 3 (top).

5.1. Spectrum cartography

When designing the basis functions in (1), it is known a priori that the transmitted signals are indeed normalized raised cosine pulses with center frequencies f_c on a grid of 10 evenly spaced points in B, with roll-off factors $\rho \in \{0, 1\}$, and bandwidths $W \in \{10, 20, 30\}$ MHz. However, the actual combination of bandwidths and roll-off factors used can be unknown, which justifies why an overcomplete set of bases comes handy. This setup amounts to 60 possible combinations for ρ, W, and f_c, thus $N_b = 60$ bases are adopted. Each CR computes periodogram samples $\hat{\phi}_{rn}(\tau)$ at $N = 64$ frequencies with $SNR = -5$ dB, and averages them across $T = 1000$ time-slots to form $\varphi_{rn},\ n = 1, \ldots, 64$ as in (3). These network-wide observations at $T = 1000$ are collected in $\boldsymbol{\varphi}$, and following steps S1-S4 at the end of Section 4, the spline-based estimator (4), and

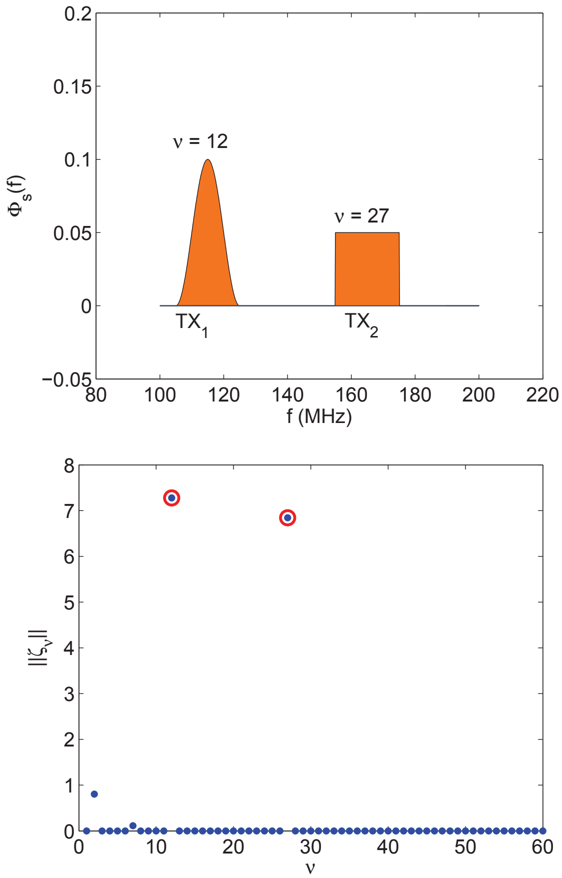

Fig. 2. (top) PSD generated by both sources; (bottom) frequency bases selected by the nonparametric basis pursuit estimator.

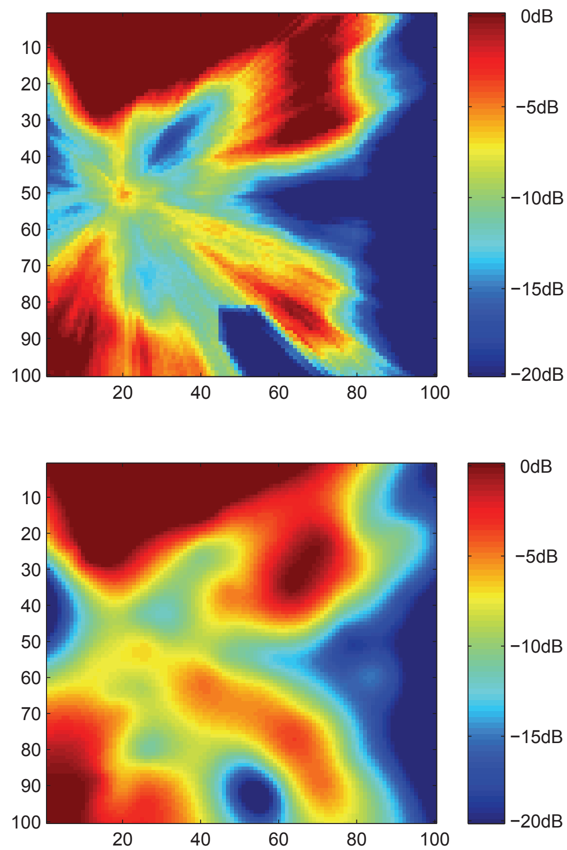

Fig. 3. (top) RF propagation generated by TX_1; (bottom) estimated field $\hat{g}_{12}(\mathbf{x})$.

thus the PSD map $\hat{\Phi}(\mathbf{x}, f)$ is formed. The estimated factor $\hat{g}_1(\mathbf{x})$ is depicted in Fig. 3 (bottom). Inspection of the estimate $\hat{\Phi}(\mathbf{x}, f)$ across frequency confirms that group-Lasso succeeds in selecting the candidate bases. Fig. 2 (bottom) shows points representing $\|\hat{\boldsymbol{\zeta}}_\nu\|_2$, $\nu = 1, \ldots, N_b$, where $\hat{\boldsymbol{\zeta}}_\nu$ is the sub-vector in the solution of the group-Lasso estimator (6) associated with $g_\nu(\mathbf{x})$ and $b_\nu(f)$. They peak at indexes $\nu = 12$ and 27 (circled in red), which correspond to the "ground-truth" model, since bases b_{12} and b_{27} match the spectra of the transmitted signals.

In summary, this test case demonstrates that the spline-based estimator can reveal which frequency bands are (un)occupied at each point in space, thus allowing for spatial reuse of the idle bands. For instance, transmitter TX_1 at the left in Fig. 3 is associated with the basis function $b_{12}(f)$, the only one of the transmitted two that occupies the $105 - 125$ MHz sub-band. Therefore, this sub-band can be reused at locations $\mathbf{x}$ away from the transmission range of TX_1, which is represented by the blue area in Fig. 3.

6. REFERENCES

[1] P. Agrawal and N. Patwari, "Correlated link shadow fading in multihop wireless network," *IEEE Trans. Wireless Communications*, vol. 8, no. 8, pp. 4024 – 4036, Aug 2009.

[2] S. Barbarossa, G. Scutari, and T. Battisti, "Cooperative sensing for cognitive radio using decentralized projection algorithms," in *Proc. of SPAWC*, Perugia, Italy, Jun. 2009, pp. 116 – 120.

[3] J. A. Bazerque and G. B. Giannakis, "Distributed spectrum sensing for cognitive radio networks by exploiting sparsity," *IEEE Trans. on Signal Processing*, vol. 58, pp. 1847–1862, Mar. 2010.

[4] J. A. Bazerque, G. Mateos, and G. B. Giannakis, "Group-lasso on splines for spectrum cartography," *IEEE Trans. Signal Processing*, June 2010 (submitted); also arXiv:1010.0274v1 [stat.ME].

[5] S. S. Chen, D. L. Donoho, and M. A. Saunders, "Atomic decomposition by basis pursuit," *SIAM Journal on Scientific Computing*, vol. 20, pp. 33–61, 1998.

[6] J. Duchon, *Splines Minimizing Rotation-Invariant Semi-norms in Sobolev Spaces*. Springer-Verlag, 1977.

[7] Y. Lin and H. H. Zhang, "Component selection and smoothing in multivariate nonparametric regression," *Annals of Statistics*, vol. 34, pp. 2272–2297, May 2006.

[8] K. Nishimori, R. D. Taranto, H. Yomo, P. Popovski, Y. Takatori, R. Prasad, and S. Kubota, "Spatial opportunity for cognitive radio systems with heterogeneous path loss conditions," in *Proc. of 65th Vehicular Technology Conference*, Dublin, Ireland, Apr. 2007, pp. 2631–2635.

[9] Z. Quan, S. Cui, V. H. Poor, and A. H. Sayed, "Collaborative wideband sensing for cognitive radios," *IEEE Signal Processing Magazine*, vol. 25, pp. 60–73, Nov. 2008.

[10] M. Yuan and Y. Lin, "Model selection and estimation in regression with grouped variables," *J. Royal. Statist. Soc B*, vol. 68, pp. 49–67, 2006.